Available online at www.sciencedirect.com
SCIENCE DIRECT
Cement and Concrete Research 36 (2006) 492–503
Cement and Concrete Research

In situ leaching method for determination of chloride in concrete pore water

L. Cáseres [a,*], A.A. Sagüés [a], S.C. Kranc [a], R.E. Weyers [b]

[a] Department of Civil and Environmental Engineering, University of South Florida, Tampa, FL 33620, USA
[b] Department of Civil and Environmental Engineering, Virginia Polytechnic Institute and State University, Blacksburg, VA 24061, USA

Received 13 July 2005; accepted 13 December 2005

Abstract

In the in situ leaching (ISL) method, pore water ionic content is determined in small cavities drilled in mortar/concrete specimens. Prior investigations have demonstrated the ISL applicability to obtain pH and nitrite ion concentration in concrete/mortar pore water. The application of the method is extended here to determine pore water chloride ion concentration (and pH) within practical test times in mortars and concretes prepared in the laboratory and in concrete cores extracted from a bridge deck in deicing salt service. Spatial resolution for the determination of composition profiles is also illustrated. Modeling of the ISL process indicates that chloride binding accelerates the approach toward a terminal cavity concentration, reducing test duration to practical lengths for moderate permeability concretes. This acceleration can be attributed to maintaining a higher gradient of free chloride near the cavity wall due to the release, during leaching, of previously bound chloride. Consequently, there is a faster chloride buildup in the cavity water compared with the no-binding case. Experimental chloride and pH results obtained by the ISL test in mortar samples show good agreement with those from the pore water expression (PWE) method. Also, examples are presented of application of ISL data to obtain chloride binding isotherms, and pore water chloride to hydroxide ratio relevant to assessing conditions for corrosion of steel reinforcement. The ISL method presents a less costly and less disruptive alternative to PWE for pore water analysis. It is noted, however, that in a few instances ISL could not be implemented because of excessive absorption of cavity water by the surrounding medium.

Keywords: Chloride; Leaching; Binding; Corrosion; Pore water

1. Introduction

Significant interest exists in assessing concrete pore water composition, particularly for chloride content as a source of corrosion of reinforcing steel. The most common procedure for assessment of cement paste/mortar pore water composition is by the use of the pore water extraction (PWE) technique, although it may be subject to errors, especially when applied to concrete samples [1–4]. Moreover, the PWE method requires special safety precautions and is highly mechanically disruptive of the concrete/mortar sample.

As an alternative to the PWE method, Castellote et al. [5] developed an alkaline leaching technique for free chloride analysis of a crushed concrete/mortar specimen in about 24 h of testing. However, this method is also highly disruptive of the sample. Glass and Buenfeld [2] determined free chloride content of a thin cement paste disk immersed in a NaCl–NaOH solution placed in an ultrasonic bath. The chloride concentration was determined measuring the external solution concentration evolution with time until an apparent terminal chloride value was reached, typically after 14 days. The practical implementation of this method with actual concrete samples has yet to be demonstrated.

The in situ leaching (ISL) technique represents another attractive practical alternative to determine pore water chloride content, but its applicability needed to be explored. ISL was initially developed to measure pH of the concrete/mortar pore water [6], and later implemented to examine nitrite concentration in concrete pore water [7]. In the ISL technique a mortar/concrete specimen is allowed to reach near water saturation in a closed 100% relative humidity chamber, periodically mist spraying the specimen surface with distilled water. Fresh lime is placed inside the chamber to act as a CO_2 trap. After 30–40 days of conditioning, small equidistant cavities (typically 3–5

* Corresponding author. Tel.: +1 813 974 8899; fax: +1 813 974 2957.
E-mail address: lcasere2@eng.usf.edu (L. Cáseres).

0008-8846/$ - see front matter © 2005 Elsevier Ltd. All rights reserved.
doi:10.1016/j.cemconres.2005.12.013

mm diameter, 30–40 mm deep and at least 20 mm apart) are drilled with minimum disruption of the specimen using a masonry drill bit. Concrete dust is carefully removed from cavities. An acrylic washer is then affixed to the rim of each drilled cavity with a fast curing epoxy. Subsequently, a small volume (typically 0.25 mL) of distilled water is injected. The cavity-to-water volume ratio is made as large as practicable to shorten the test period. A rubber stopper is firmly pushed into the acrylic washer to isolate the cavity water. The cavity water is then allowed to evolve toward equilibrium with the surrounding pore water over a sufficiently period of time. Periodically, a small amount of cavity water (10–30 mg) is extracted and analyzed for dissolved species.

The ISL method is inexpensive, simple to implement in concretes (of high and moderate permeability) and mortars, and causes minimum disruption. Loss of cavity water into the surrounding concrete and a potentially lengthy required time toward cavity water equilibration are limitations of the technique.

This investigation was conducted to evaluate the applicability of the ISL method for the determination of chloride in mortar/concrete pore water. Of interest was whether test times could be kept within reasonable limits in view of the often moderate diffusivity of chloride ion in concrete [8,9], and how chloride binding [10,11] may affect the cavity water equilibration kinetics. These issues were addressed by detailed modeling to examine equilibration kinetics. Results using the ISL technique are compared with those obtained by the well-established PWE method applied to mortar samples. The applicability of the ISL technique to obtain a chloride distribution and binding information pertinent to durability forecasting is demonstrated.

1.1. Modeling of chloride transport into small concrete cavities

The success of the ISL method depends on the development within the cavity, in a reasonable timeframe, of a chemical composition representative of that of the surrounding pore water. Early modeling work [6] of the approach to equilibration addressed only simple diffusion with no binding of the type often encountered for chloride transport in concrete. Those results indicated that the time needed to achieve near equilibrium is proportional to $D^{-1}r_c^2$ and roughly proportional to $\varepsilon^{-2}V_r^{-2}$, where r_c is the cavity radius, D the diffusion coefficient (binding absent) of the leached species, ε the porosity (pore volume fraction) of the material, and V_r is the ratio of the cavity volume V_C to the volume of water in the cavity V_W. This analysis permitted semi-quantitative projections of the time for equilibration in the more complex systems of interest. Those projections together with experimental results showed encouragingly short times (e.g. one week) for equilibration for ions responsible for pH development [6]. Additional work with nitrite ions showed also reasonable short times to approach equilibrium [7]. The present paper extends the model to the transport of chloride ions including linear and non-linear binding.

For modeling purposes, the following assumptions are made:

1. The concrete cavity is treated as a long cylinder of length L and a radius r_c centered in a cylindrical specimen also of length L (thus, chloride transport beneath the cavity is ignored for simplicity) and radius $r_e \gg r_c$ (see Fig. 1). The chloride concentration at $r=r_e$ is assumed to be unaffected by leaching within the time frame of the experiment. Chloride is initially uniformly distributed in the concrete matrix.
2. The concrete pores are assumed to be always filled with water so that cavity water depletion is negligible (limitations for the applicability of this assumption are discussed later).
3. The concrete is considered as a homogeneously porous medium with porosity invariant with time.
4. The cavity is assumed to be partially filled with water but with walls efficiently wetted by capillarity.
5. Transport inside the cavity is assumed to be fast enough so as to have the same chloride concentration in the water at the bottom and on the moist cavity walls.
6. Equilibrium between the cavity and concrete pore water is reached at the cavity wall at all times.
7. The total chloride content as mass per unit volume of concrete can be expressed as $C_{TOT}=C_B+C_F$, where C_B is the bound chloride and C_F is the free chloride. The free chloride is present only in the pore water at concentration C_f (in mass per unit volume of pore water), so that:

$$C_F = \varepsilon \cdot C_f \tag{1}$$

8. There is instantaneous equilibration between bound and free chlorides so that C_B and C_F are related by a time-invariant isotherm function.
9. Chloride transport in the bulk of the concrete is by diffusion, forced only by gradient of the free chloride concentration.

In one-dimensional cylindrical coordinates, the mass conservation equation for chloride transport in the concrete bulk is then given by [10,12]:

$$\frac{\partial C_F}{\partial t} = \frac{D_F}{\left(1+\frac{dC_B}{dC_F}\right)}\left[\frac{\partial^2 C_F}{\partial r^2}+\frac{1}{r}\frac{\partial C_F}{\partial r}\right] \tag{2}$$

where r is the distance from the center of the cavity, D_F is the diffusion coefficient for free chloride, dC_B/dC_F is given by the binding isotherm, and t is the leaching time.

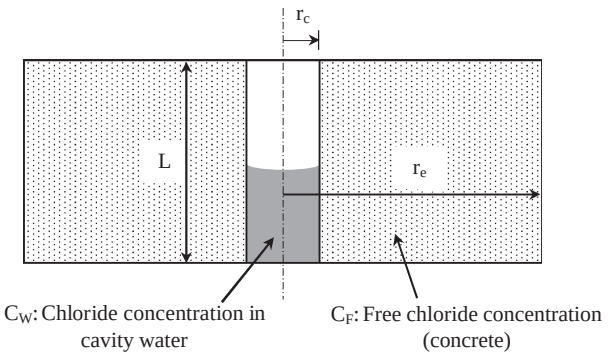

Fig. 1. Schematic for simplified modeling of chloride transport — only radial transport considered.

The chloride mass flowing per unit time into the cavity, dm/dt, is given by Fick's first law evaluated at the cavity wall:

$$\frac{dm}{dt}|_{r=r_c} = 2 \cdot D_F \cdot \pi \cdot r_c \cdot L \cdot \frac{\partial C_F}{\partial r}|_{r=r_c} \quad (3)$$

Since $V_C = \pi r_c^2 L$, the chloride concentration in the cavity water in mass per unit volume of liquid, C_W, at the cavity wall varies with time as:

$$\frac{dC_W}{dt}|_{r=r_c} = \frac{2 \cdot D_F \cdot V_r}{r_c} \cdot \frac{\partial C_F}{\partial r}|_{r=r_c} \quad (4)$$

Substituting Eq. (1) into Eq. (4) and recalling that the cavity water is assumed to be in equilibrium with the pore water at the cavity walls at all times yields the condition:

$$\frac{dC_F}{dt}|_{r=r_c} = \frac{2 \cdot D_F \cdot \varepsilon \cdot V_r}{r_c} \cdot \frac{\partial C_F}{\partial r}|_{r=r_c} \quad (5)$$

The other conditions consistent with the model assumptions are:

$$C_F(r_c, 0) = \varepsilon \cdot C_{W0} \quad (6a)$$

$$C_F(r, 0) = C_{F0} \quad (6b)$$

$$C_F(r_e, t) = C_{F0} \quad (6c)$$

where C_{F0} is the initial free chloride concentration in concrete and C_{W0} is the initial chloride concentration in the cavity water. Since chloride-free water is initially injected, C_{W0} is zero.

The time evolution of the chloride concentration in the cavity water can then be obtained by solving Eq. (2) with the conditions in Eqs. (5) and (6a)–(6c). The problem can be expressed in non-dimensional terms by substituting C_F, t, and r by the dimensionless parameters:

$$C_G = \frac{C_F}{C_{F0}} = \frac{C_f \cdot \varepsilon}{C_{F0}} \text{ (Generalized Concentration)} \quad (7a)$$

$$T = \frac{D_F}{r_c^2} \cdot t \text{ (Generalized Time)} \quad (7b)$$

$$R = \frac{r}{r_c} \text{ (Generalized Distance)} \quad (7c)$$

This formulation permits easy comparison of the ISL behavior in the presence or absence of binding. Chloride binding in concrete was modeled by the Langmuir isotherm described by $C_B^{-1} = (KC_F)^{-1} + C_L^{-1}$ where K and C_L are the Langmuir constant adsorption parameters. However, this choice is not limiting and other adsorption isotherms can be used instead [2,13]. Using the non dimensional parameters, the term dC_B/dC_F in Eq. (2) becomes:

$$\frac{dC_B}{dC_F} = \frac{K}{\left(1 + \frac{K \cdot C_{F0}}{C_L} \cdot C_G\right)^2} \quad (8)$$

Defining the non dimensional groups $\beta = KC_{F0}C_L^{-1}$ and $\gamma = \varepsilon V_r$, Eq. (2) becomes:

$$\frac{\partial C_G}{\partial T} = \frac{1}{1 + \frac{K}{(1+\beta \cdot C_G)^2}} \cdot \left(\frac{\partial^2 C_G}{\partial R^2} + \frac{1}{R}\frac{\partial C_G}{\partial R}\right) \quad (9)$$

and the problem conditions in non-dimensional terms become:

$$\frac{dC_G}{dT}|_{R=1} = 2 \cdot \gamma \cdot \frac{\partial C_G}{\partial R}|_{R=1} \quad (10)$$

$$C_G(1, 0) = 0 \quad (11a)$$

$$C_G(R, 0) = 1 \quad (11b)$$

$$C_G(R_e, T) = 1 \quad (11c)$$

Fig. 2 shows solutions to Eqs. (9) (10) (11a) (11b) (11c) numerically calculated using finite differences for a typical configuration where $\gamma = 0.3$ (e.g. $\varepsilon = 0.1$, $V_r = 3$). Calculations are presented for (i) a no binding case ($K = 0$) and several binding scenarios all assuming $K = 10$, which is in the order of values reported in the literature [14–17] and comparable to those obtained with the materials used here. In the first binding scenario (ii) conditions are assumed to be at the linear limit ($C_L = \infty$, so $\beta = 0$) approximating the behavior that may occur if C_{F0} were vanishingly small compared to the bound chloride content in the bulk of the specimen. The remaining binding scenarios were chosen with $\beta = 0.25$ (iii), 1.25 (iv), and 7.5 (v) representing cases in which the ratio of free to bound chloride content in the bulk of the specimen is finite but small (0.12), moderate (0.22), or approaching unity (0.85), respectively.

In all instances the approach to equilibration is measured by the increasing value of $C_G(1, T)$ as T increases. The scaling of T in Eq. (7b) implies that the time to reach a given fraction of the terminal concentration should be inversely proportional to D_F and r_c^{-2}, as indicated earlier. For the no-binding case the results (curve (i)) are generally as reported by Sagüés et al. [6]. The present curve represents a refined numerical calculation scheme yielding more accurate values at low values of T than in Ref. [6]. Since for linear binding dC_B/dC_F is a constant, the ruling equations and end conditions are directly scalable to those of the no-binding case. Comparison between those cases is then straightforward and it shows marked acceleration (by a factor of $\sim(1+K)$ if D_F remains the same, see below) in the evolution of C_G toward unity when linear binding is present (curve (ii)). This finding would at first glance seem inconsistent with the commonly observed retarding effect of binding on chloride penetration in concrete [12]. The apparent discrepancy is

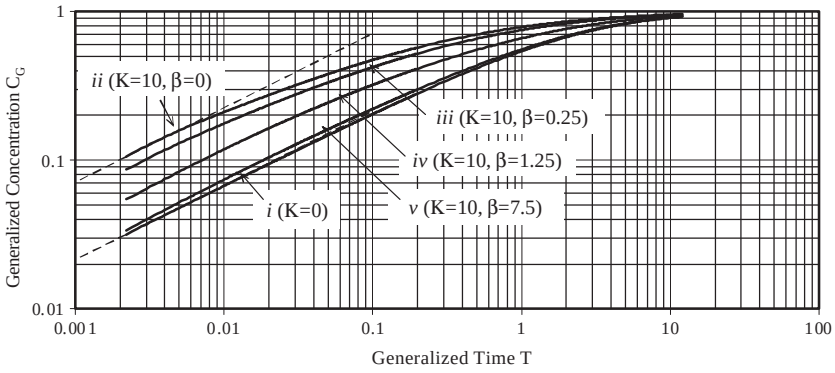

Fig. 2. Non dimensional model results (γ=0.3).

explained however by noticing that during leaching the release of previously bound chloride permits maintaining a high gradient of C_F near the cavity wall for a longer time than otherwise, thus actually accelerating the buildup of chloride in the cavity water.

For the no-binding and linear binding cases the chloride buildup at short leaching times is amenable to simplified treatment. Early on diffusional transport can significantly deplete only a very thin region around the cylindrical cavity surface, so the behavior closely resembles that of diffusional leaching from a flat wall into a reservoir of large but finite volume. Adapting the well known solution for that case [18] to the present system yields $C_G \sim 4\pi^{-1/2}\gamma\,(1+K)^{1/2}T^{1/2}$. The result is described by the dashed straight lines (at low T) with slope 1/2 in the log–log representation used in Fig. 2. The lines agree with the limit behavior of the respective numerical solutions and coincide in showing an accelerating factor $(1+K)$ in the earlier leaching stages due to non-linear binding.

The behavior for the non-linear binding cases depends strongly on the ratio of free to bound chloride in the bulk. If the ratio is very small (which occurs when $C_F \ll C_L$ as in case (iii)) then the entire specimen exists in a regime close to the linear limit of the Langmuir isotherm. Thus the calculated approach to equilibrium in such case closely resembles, as expected, that of the linear binding case. However, a moderate increase in the free-to-bound chloride ratio in the bulk as in case (iv) results in a response halfway (in logarithmic terms) between that of the no-binding and linear binding limits. When the free-to-bound chloride ratio in the bulk becomes near unity the response (curve (v)) is already close to that of the no-binding case. It is noted that the initial log–log slope in these cases is also in the order of 1/2 in keeping with the diffusional transport assumptions. A limit correlation of the vertical offset with the diffusivity and binding parameters for the non linear case (comparable to that introduced above for the linear/no binding cases) is still under investigation.

The model results indicate that chloride binding does not slow down the approach to equilibration between cavity and pore water, and that instead binding may provide substantial acceleration in some cases. However, application of the model to estimate the test duration needed to get reasonably close to C_{F0} is difficult because measured chloride diffusion coefficients in concrete are typically reported as apparent values, D_{APP}, instead of D_F. Those D_{APP} values are obtained by fitting an ideal error function solution of the diffusion problem to measured profiles of total or near-total chloride concentration of the form [19,20]:

$$C_{TOT}(x,t_c) = C_S \cdot \left(1-\mathrm{erf}\left(\frac{x}{2\sqrt{D_{APP}\cdot t_c}}\right)\right) \quad (12)$$

where x is the distance from the concrete surface exposed to salting, t_c is the concrete exposure time to salting, C_S is the chloride concentration at the concrete surface assumed to be approximately constant in time, and the native concentration deep in the core is assumed to be negligible. An approximation can nevertheless be made by assuming Langmuir binding and noting that by analogy with the above arguments the value of D_F should be somewhere between $(1+K)$ D_{APP} and D_{APP}, depending on the overall chloride content in the samples that were used to calculate D_{APP}. Additional complexity results from factors such as dependence of D_F on time [18] and concrete heterogeneity near the surface which are beyond the scope of the present discussion.

As an illustration, one can consider values of $D_{APP} \sim 10^{-12}$ m^2/s which are often reported for relatively moist moderate permeability concretes [8,9]. In the complete absence of binding or with very high chloride levels throughout then $D_F \sim D_{APP}$ so a curve approaching (i) in Fig. 2 would apply for practical cavity dimensions. The time required to attain a sizable fraction (e.g. C_G=0.8) of the terminal chloride content in the cavity water would then be quite long (~6 months). But binding to a significant extent is always likely to exist and chloride content is

Table 1
Mortar mix proportions

Mixes	Mix B				Mix A	
Series name	Series T				Series S	
Batch name	M05T	M1T	M3T	M5T	M10S	M20S
Cement, kg/m^3	504	501	496	489	484	469
Water, kg/m^3	252	251	248	244	193	188
w/c ratio	0.5	0.5	0.5	0.5	0.4	0.4
Fine aggregate, kg/m^3	1386	1378	1363	1343	1330	1290
Target C_{TOT}, kg/m^3	2.5	5.0	14.9	24.5	8.6	16.7
Unit weight, kg/m^3	2152	2145	2144	2126	2122	2108

finite, so behavior not unlike (iii) or (iv) may be closer to the norm. Moreover, since T is scaled by D_F and not D_{APP}, the approach to equilibration is accelerated in the actual time domain (compared to the case of $D_F \sim D_{APP}$) not only by the shift from (i) to (v), (iv) etc. but also by an added factor of D_F/D_{APP}. In this illustration behavior as in (iv) would reduce the time to achieve $C_G = 0.8$ to only ~1 month. In more highly permeable concretes or in mortars near-equilibration times would be even shorter, suggesting a good potential for rapid test execution in a variety of problems of interest. Experimental tests of the feasibility and validity of the method in mortars and concretes are presented in the following sections.

2. Experimental methodology

A note on unit usage: In the following, concentrations related to concrete mixture proportions are given in customary kilograms per cubic meter form. For consistency with usual analytical practice, concentrations of solutions are given in moles/liter (M) units instead. Appropriate conversion needs to be made when relating pore water and bulk concrete compositions e.g. by volumetric porosity.

2.1. Laboratory mortar specimens

Two mortar mixes (A and B, Table 1) were prepared following ASTM C-305-94. Mix A was cast in cylindrical plastic molds 4 cm diameter by 25 cm long (series S) with a nominal water-to-cement (w/c) ratio of 0.4. Mix B (series T) was cast in plastic molds 7.6 cm diameter by 15.2 cm long with a nominal w/c ratio of 0.5. Chloride ions were introduced as part of the mixing water, using reagent grade NaCl (99.4% purity) to attain the desired total chloride concentration (C_{TOT}) obtained by the method detailed in [21]. This method yields acid-soluble chloride and is comparable with ASTM C1152-90. Mortar cylinders were prepared in duplicate for each C_{TOT} value. The fine aggregate was Ottawa sand graded per ASTM C-778 that had an absorption capacity of 0.2% and water content of 0.9%. The sand-to-cement ratio was 2.75 in all cases. Companion mortar samples were used to determine the volumetric porosity per ASTM C-642-90 adapted for a small size sample. Both mixes used Type I Ordinary Portland cement with chemical oxide composition shown in Table 2.

The cylinders were demolded 18 h after casting and cured inside a closed ~100% relative humidity (RH) chamber for 30 days, occasionally lightly mist spraying with distilled water the mortar surface. Following curing, the series S and T cylinders were transversely cut (~60 mm long for series S and ~62 mm long for series T) for the ISL and PWE tests. After 30 days of conditioning, three equidistant cavities (3.6 mm diameter and 35 mm deep) were drilled perpendicular to the newly cut cross-section of series T specimens as shown in Fig. 3, whereas two cavities (3.6 mm diameter and 25 mm deep) were drilled on the lateral surface of the series S specimens, using a masonry drill bit in all cases. Next, the cavities were carefully cleaned to remove all traces of dust and a Plexiglas washer was attached with epoxy adhesive to the rim of each cavity. A volume of 0.22 cm^3 ($V_r = 1.16$ and 1.62 for series S and T, respectively) of distilled water was then injected into each cavity, and a rubber stopper was pressed firmly into the washer to minimize contact with the external environment. The specimens were kept inside a 100% RH chamber at ~22 °C during the ISL test evolution.

The PWE method similar to that described by Barneyback and Diamond [22] was implemented with the mortar samples. A steel piston inserted into a 19 mm bore was used to apply a maximum nominal pressure of ~400 MPa after ~5 min and maintained at that pressure for ~15 min. The mortar sample (~15 g) was crushed by hammering into ~10 mm pieces. About 0.5 mL, which represented ~40% of the total mortar pore water, were typically squeezed out and collected with a syringe connected to an opening at the bottom of the bore. The expressed solutions were tested for chloride and pH in the same manner as those sampled from the cavities in the ISL method.

2.2. Laboratory concrete specimens

The concrete specimens were cored out of six simulated concrete bridge deck slabs 118 × 118 × 21.6 cm prepared with Type I Ordinary Portland cement and various amounts of NaCl introduced as part of the mixing water. The mixture proportions and materials used for the preparation of the laboratory concrete slabs (Table 3) represented Virginia Department of Transportation (VDOT) requirements for typical bridge deck applications [23] and were reasonably comparable to those specified for the bridge deck under evaluation. The C_3A content was ~10.2% by weight of cement. The coarse aggregate was crushed limestone with an absorption capacity of 0.62%, and the fine aggregate was siliceous natural sand. The slabs were exposed horizontally outdoors in Blacksburg, Virginia for ~8 years, after which concrete cores, ~10 cm diameter and ~17 cm long, were extracted by drilling perpendicular to each slab, and archived in airtight plastic wrapping for ~1 year awaiting evaluation. The cores were then stripped and placed for conditioning in a ~100% RH chamber for 40 days at ~22 °C. Slices 2 cm thick were cut out of the bottom of each core for porosity and C_{TOT} measurements determined as noted above. In the remainder of the core, four aligned cavities (0.36 cm diameter, 3.5 cm deep and 2 cm separation) were drilled perpendicular to the lateral surface following the same practice as in the mortars, and 0.30 cm^3 of distilled water were injected into each cavity.

Table 2
Chemical analysis of the Type I Ordinary Portland cements (% wt cement)

Analysis	CaO	SiO_2	Al_2O_3	Fe_2O_3	Na_2O	K_2O	SO_3	C_3S	C_2S	C_3A	C_4AF
Mix A	66.2	21.4	3.85	3.49	0.10	0.15	2.43	69.1	9.61	4.31	10.6
Mix B	65.5	21.1	4.32	4.25	0.06	0.10	2.61	63.4	13.1	4.25	12.9

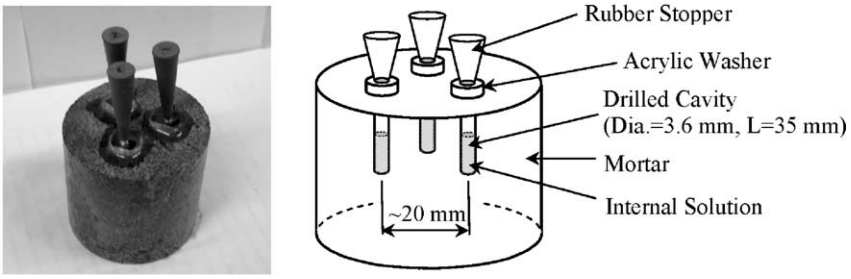

Fig. 3. External appearance and schematic of the ISL arrangement for series T specimens.

2.3. Field-extracted concrete specimens

Three specimens (~10 cm diameter and ~15 cm long; Table 5) were cored from a 12-year old deck of bridge No. 1015 in Salem District 2 in Virginia, exposed to deicing salt service. That construction class included a maximum 0.45 w/c specification with no pozzolanic additions. As noted above, the mixture proportions and materials specified were similar to those shown in Table 3. The cores, archived in airtight plastic wrapping for ~1 year awaiting evaluation, were stripped and placed for conditioning in a ~100% RH chamber for 40 days at ~22 °C. Eight cavities, 0.36 cm diameter and 3.5 cm deep, were drilled as shown in Fig. 4. The cavities were positioned at different distances measured from the core end face that corresponded to the roadway surface, directly exposed to salting. Afterwards, 0.22 cm^3 of distilled water were injected in each cavity. The cutout used for C_{TOT} analyses was transversely cut in ~1.2 cm thick slices with a diamond saw, matching the center of each cavity. Volumetric porosity was determined as above using the 4 cm thick cutouts shown in Fig. 4.

2.4. pH and chloride concentration in ISL cavities

To determine chloride content in the cavity, ~0.01 to 0.03 g of solution (sampling a different cavity on a rotating schedule at the end of each time interval) were periodically extracted with a glass pipette. Sample mass was determined to a precision of 0.1 mg. When necessary, mass to volume conversions were made correcting for liquid density estimated from ionic content. Chloride concentrations were usually determined by potentiometric titration with silver nitrate with appropriate blank controls. For low chloride concentration samples a Dionex DX-600 ion-exchange chromatograph was used, fed with 9 mM Na_2CO_3 eluent at 1 mL/min. For the laboratory specimens, typically two cavity water chloride measurements were conducted during the first week, sampling one cavity each time. After the first week, cavity water chloride measurements were performed once a week. For the field specimens, extractions from one cavity at each depth were conducted using the same methodology as in the laboratory samples.

Cavity water pH was monitored with a glass pH microelectrode (model MI-405 from Microelectrodes, Inc.) inserted momentarily in the cavity and a silver–silver chloride (Ag–AgCl) reference microelectrode (model MI-402) connected to a high input impedance pH meter set as voltmeter. Both microelectrodes had a 2 mm external diameter. The microelectrodes were calibrated using pH 10, 12, and 13 buffer solutions corrected by the appropriate solution temperature factor. Due to the small cavity diameter, one of the cavities of each specimen was always used for the reference electrode insertion while the pH electrode was inserted in the other cavities. Determination of cavity pH using the ISL method is given in detail in Sagüés et al. [6].

The periodic sampling for chloride determination caused modest cavity water depletion as time progressed, but in some cases faster water loss was encountered. Since the stopper prevented evaporation, the extra loss could only take place into the surrounding concrete where water saturation during the conditioning period may have been incomplete. The extra water loss was severe in some cases, resulting in an empty cavity after a period ranging from days to weeks from the moment water was first inserted. If at the time of the test one or more of the cavities were found to be empty, the water sample was extracted from a peer cavity that still had solution. The empty cavity was recharged with fresh water to the initial volume, and not monitored until a subsequent scheduled time. For cavities that did not become empty throughout the test, leaching time was counted from the moment of initial water addition. For cavities that became empty and were recharged leaching time was reset to zero at the moment of water recharge. The data from subsequent replenishments were treated as if starting afresh, and evaluated together with previous results from the same cavity.

3. Results and discussion

3.1. Material characterization

Tables 4 and 5 report the volumetric porosity and the C_{TOT} results for all specimens. The porosity values, including the high

Table 3
Laboratory concrete mix proportions

Specimen	0-1	6-1	12-1	24-1	48-1	96-1
Cement, kg/m^3	381	381	379	379	379	382
Water, kg/m^3	173	160	159	155	167	162
w/c ratio	0.45	0.42	0.42	0.41	0.44	0.43
Target C_{TOT}, kg/m^3	0.0	0.4	0.7	1.4	2.9	5.7
Fine aggregate, kg/m^3	718	718	718	706	712	713
Coarse aggregate, kg/m^3	1068	1068	1037	1079	1067	1078
Unit weight, kg/m^3	2232	2196	2148	2232	2232	2139

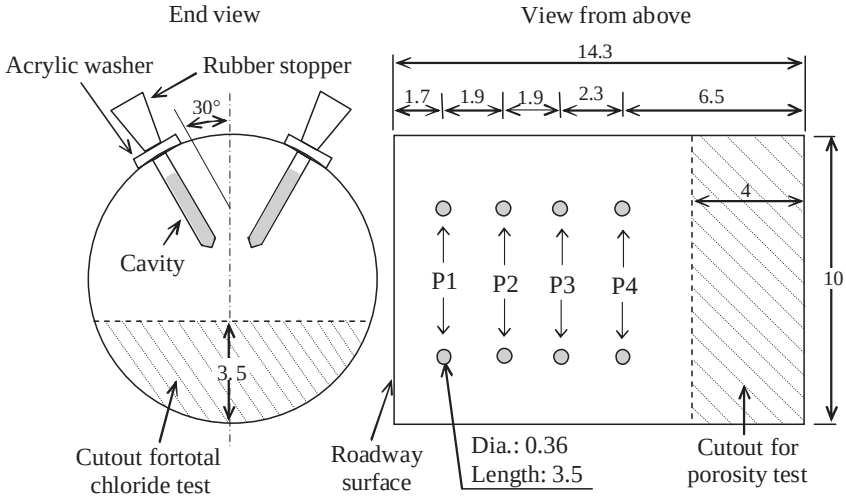

Fig. 4. Schematic of the arrangement for the field specimen A1 (dimensions are in centimeters).

porosities recorded for the mortar specimens, are typical of those commonly reported for materials with similar mixture proportions to those used here. The C_{TOT} results of the laboratory concrete specimens generally reflected the admixed amounts and are expected to have been little affected by weathering at the depths where the ISL cavities were placed. The field concrete cores exposed to salting showed a distinct C_{TOT} gradient as function of depth (Table 5). Applying Eq. (12) to the C_{TOT}-depth profiles, the resulting D_{APP} values (Table 5) are in the order of 2–4 10^{-12} m^2/s, typical of concretes of moderate to high permeability. This outcome is consistent with the mixture proportioning of the laboratory concretes (assumedly similar to that of the field samples, and likely to have shown comparable results if similarly exposed) which had modest w/c ratio and cement factor, as well as no pozzolanic addition [8,24]. The laboratory mortars, with even higher w/c ratio and their high observed porosity, would be expected to have yielded even higher D_{APP} values under similar conditions.

3.2. ISL general trends and spatial resolution

The theoretical model, although highly simplified, yielded encouraging projections as to the applicability of the ISL method to determine free chloride in concrete/mortar of moderate permeability, and predicted that chloride binding is beneficial in accelerating the test. However, aspects of the problem, such as the effect of loss of cavity water into the surrounding concrete when water saturation is less than complete are not covered by the present model, and need to be considered in future analysis.

Figs. 5, 6, and 7 show the evolution of C_W with leaching time for up to 110 days for the mortars, laboratory concretes, and field specimens, respectively. Each data point represents the value for a particular cavity of each specimen at a given leaching time. Replicate specimens showed comparable results and there was clear differentiation between the various test conditions. As time progressed, chloride concentration in cavity water approached an apparent terminal concentration (denoted as C_{WT} hereafter) which was larger the greater the total admixed chloride content in the specimen. This correlation can then be used to estimate binding relationships as it will be shown below. For any given leaching time, all field specimens exhibited the highest C_W values in the cavities nearest the roadway surface where salt was applied. The cavities further away from that surface showed correspondingly decreasing C_W, and the C_{WT} values correlated well with the independent spatially resolved C_{TOT} evaluations shown in Table 5. The laboratory specimens showed no systematic difference in the approach toward terminal conditions for the different cavity positions, consistent with the expectation of little variation in chloride content with depth in those specimens/slabs made with admixed chlorides.

The C_{WT} value and the nominal leaching time T_D required to nearly attaining that C_{WT} for each test specimen were determined as shown in Appendix A, by tracing a single simplified fitting curve for each set of specimens based on the theoretical transport model presented above. The fitting curve consisted of a straight line of slope 1/2 for early leaching times (reflecting the near semi-infinite diffusion behavior) and a horizontal line representing attainment of equilibrium at longer

Table 4
Laboratory specimen properties

Specimen	Concretes						Mortars					
	0-1	6-1	12-1	24-1	48-1	96-1	M5T	M3T	M1T	M05T	M10S	M20S
Porosity, %	14.2	13.5	13.9	11.8	14.4	13.6	17.8	18.1	17.8	18.1	14.4	13.3
C_{TOT}, kg/m^3	0.42**	0.67	0.81	2.15	4.14	6.02	21.17	14.18	5.31	2.77	5.65	7.62*

*Excessive moisturizing of this specimen is thought to have caused partial loss of initially admixed chlorides.
**Small background level possibly reflecting mixture components contamination.

Table 5
Bridge No. 1015 field specimen properties

Specimen	Porosity, %	C_{TOT}, kg/m^3				D_{APP}, m^2/s (10^{-12})
		P1	P2	P3	P4	
A1	11.6	2.41	2.11	1.17	0.43	1.8
A2	13.7	5.17	4.03	2.34	0.80	3.2
A3	12.5	4.52	3.06	2.25	0.76	4.3

P1–P4 denotes slices centered on the cavities indicated in Fig. 4.

leaching times. The intersection of both lines takes place at $t = T_D$. The high porosity, high w/c, and absence of permeability reducing admixtures of the series T mortars was expected to facilitate chloride transport, which was confirmed by reaching an apparent terminal C_W after as little as one week of testing. Near-equilibration times were accordingly longer for the lower w/c specimens of the series S mortars. The laboratory and field concrete specimens showed stabilization times generally longer than those for the mortars but still within a practical time frame.

Water depletion substantially above the small amount extracted for analysis was encountered in some cavities of a few specimens, which were fully depleted 4 days after starting the ISL test and required multiple recharges. However, the interval between recharges became progressively longer indicative of approaching water saturation in the surrounding medium. Typically, all laboratory concretes and mortars with low admixed chloride content needed up to three cavity replenishments. On the other hand, no recharge was needed for the mortar specimens that had high admixed chloride content, which may have promoted efficient water absorption during conditioning. Loss of cavity water was notable in the case of the field specimens where useful results could not be obtained in about a third of the cases. Nevertheless, the available field specimen data illustrate the ability of ISL to obtain spatial resolution of pore water composition. Some mitigation of this problem may be achieved by allowing for an initial addition of water to the cavity (for example during the conditioning period), which would reduce the rate of absorption in subsequent fillings. Longer conditioning times to allow for thorough saturation of the test specimen may be helpful as well. These remedies may not be sufficient however for concretes that experience substantial self-desiccation during curing or that are too dense for thorough

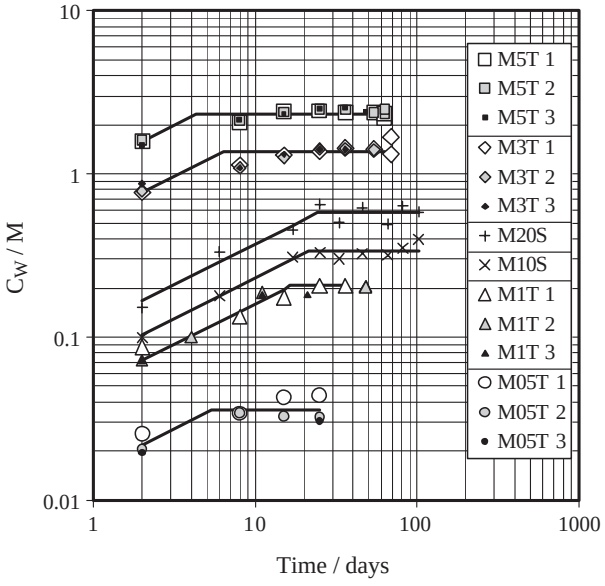

Fig. 5. Evolution of C_W with time of the mortar specimens designated per Table 1. The lines were obtained by the fitting procedure indicated in Appendix A.

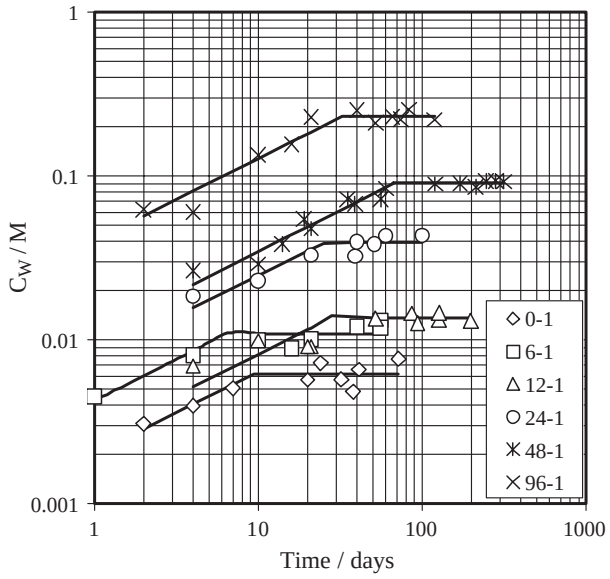

Fig. 6. C_W evolution with time and calculated trend lines for the laboratory concrete specimens listed in Table 3. The trend lines were obtained by the fitting procedure indicated in Appendix A.

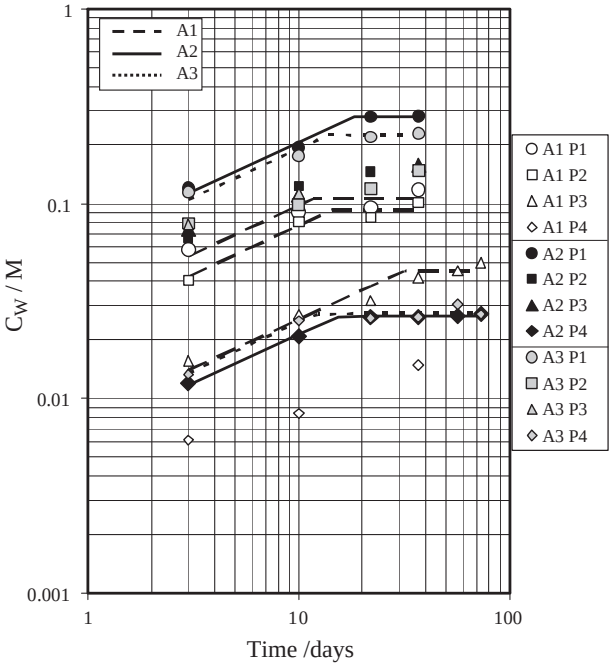

Fig. 7. C_W evolution with time and calculated trend lines for the field specimens listed in Table 5, at positions indicated in Fig. 4. Data for A1 (P4), A2 (P2–P3) and A3 (P2–P3) were not sufficient for C_{WT} evaluation. The trend lines were obtained by the fitting procedure indicated in Appendix A.

Table 6
Apparent terminal values for the laboratory specimens

Specimen	Concretes						Mortars					
	0-1	6-1	12-1	24-1	48-1	96-1	M5T*	M3T*	M1T*	M05T*	M10S	M20S
pH_T	12.98	13.12	13.15	13.01	12.83	12.63	12.22	12.53	13.14	13.35	13.11	12.97
C_{WT} (M)	0.006	0.011	0.014	0.039	0.091	0.231	2.356	1.330	0.205	0.037	0.336	0.577

*Average from data obtained from triplicate specimens.

water saturation in a practically short time. It should be noted that while ISL may not be practicable in conditions leading to excessive cavity loss, the PWE method is likewise prone to little or no water yield in dense or desiccated concrete unless the sample is first crushed to a small size and then water saturated.

Concurrent with the chloride measurements, cavity pH was monitored for up to 60 days. All specimens developed an initial high pH (~12.5), reflecting dissolution of the calcium hydroxide immediately available at the cavity wall [6]. During the first week, most specimens showed a fast increase over the initial pH and in about two weeks an apparent terminal value pH_T was reached determined as indicated in a previous publication [6]. In general, the pH_T values (reported in Tables 6 and 7) for each specimen group decreased with an increase in C_{TOT}. This effect was particularly notable in the high chloride content mortars; in the cases of M3T and M5T the pH actually decreased with time and the pH_T values were distinctly lower than the rest. As noted elsewhere, this behavior is at least in part associated with the increase in ionic strength as chloride content increases [25]. As shown in Table 7, the ISL measurements provided spatial resolution for the pH_T sequences as well in the field concrete specimens.

3.3. Agreement with PWE results

Fig. 8(a) and (b) show a comparison of the chloride and pH results obtained with the ISL and PWE techniques for mortar specimens, where PWE could be readily implemented. The terminal values matched well, over the chloride concentration and pH ranges evaluated, the results obtained by replicate PWE experiments performed on samples obtained by cutting out a representative fraction of a mortar specimen previously used for ISL implementation. These findings are consistent with similarly good agreement obtained earlier in measurements of pH by the ISL and PWE methods in concrete specimens [6] and for nitrite ion in mortar specimens [7].

3.4. Chloride binding isotherms from ISL data

Correlation of ISL results with independent measurements of porosity and C_{TOT} can provide estimates of the chloride binding isotherm of the concrete or mortar in its water-saturated condition. It is assumed that the cavity water is in equilibrium with the surrounding pore water so that $C_{WT}=C_f$, and that there is instantaneous equilibrium between C_B and C_F so that C_B is only a function of C_F. On first approximation that function is taken to be a time-invariant adsorption isotherm of the Langmuir form. Thus, a plot of C_B^{-1} as function of C_F^{-1} would show a straight line of slope K^{-1} and intercept C_L^{-1}.

For each material evaluated, C_B was obtained from the porosity test results and the data in Tables 6 and 7, by subtracting the calculated $C_F=C_{WT}\varepsilon A_W$ from C_{TOT}, where A_W is the chloride molar mass. Fig. 9 shows the resulting C_B^{-1} values as a function of C_F^{-1}. The data are grouped by combining the results from each set of specimens of similar origin i.e. series T mortars, all the laboratory concrete specimens which shared the same base mix proportions, and the three field specimens extracted from the same bridge deck. Results of the series S mortars were not evaluated since this series consisted of only two specimens. In all three groups the data arrays could be each reasonably approximated by simple linear regression, yielding values of the corresponding binding parameters K and C_L. The results are shown in Table 8 together with the range of parameters evaluated from a sampling of published results obtained using the PWE with cement pastes, mortars, and concretes of C_3A content and porosity comparable to those of the present materials. These examples are not detailed validation of the accuracy of the ISL method, but do show that the results can be precise and consistent enough to permit calculation of binding model parameter values, and that those are within reasonable bounds.

3.5. Chloride to hydroxide ratios from ISL data

The pore water hydroxide ion concentration $[OH^-]$ was estimated from Tables 6 and 7 as $[OH^-]=K_W(\gamma_{OH}10^{-pH_T})^{-1}$ where K_W is the water dissociation constant at 22 °C and γ_{OH} is the OH^- activity coefficient assumed to be ~0.7, typical of highly alkaline solutions [28]. Taking as before $C_f=C_{WT}$, the pore water chloride to hydroxide ratio $C_f/[OH^-]$ was calculated and shown in Fig. 10 as function of C_{TOT} in a log–log plot for each material group. A ratio near unity (with some correction for

Table 7
Apparent terminal values for the Bridge No. 1015 field specimens

Specimen	A1				A2				A3			
Position	P1	P2	P3	P4	P1	P2	P3	P4	P1	P2	P3	P4
pH_T	12.84	12.95	13.04	13.08	12.81	12.89	12.95	13.09	12.76	12.83	12.96	13.01
C_{WT} (M)	0.106	0.093	0.045	–	0.281	–	–	0.026	0.225	–	–	0.027

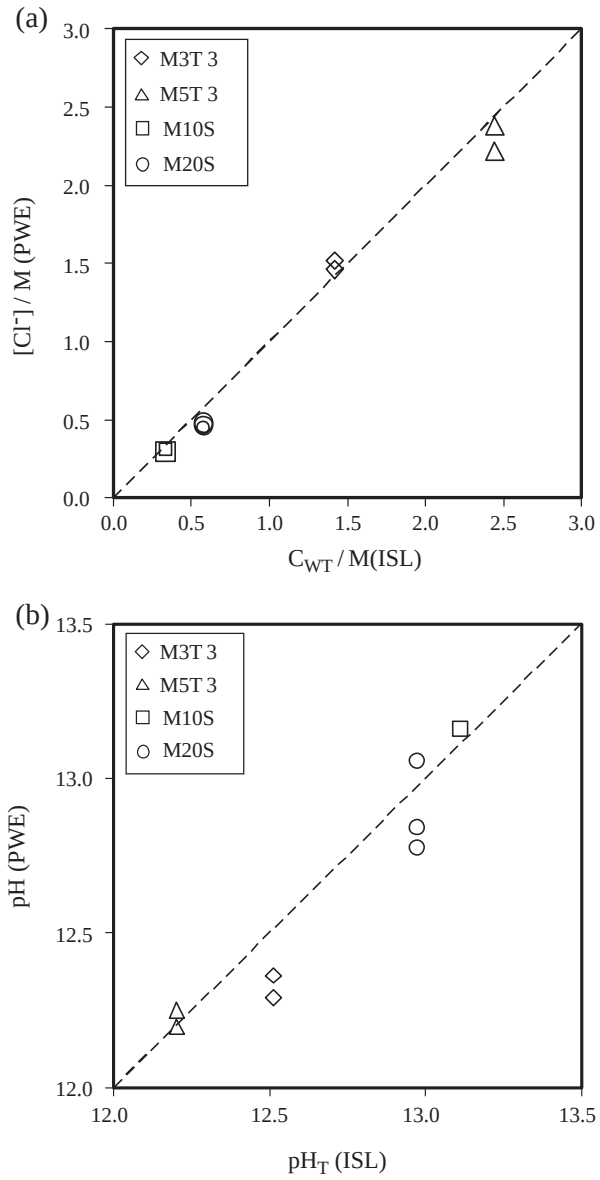

Fig. 8. (a) Chloride concentration correlation of the ISL and PWE techniques with mortar specimens. Dashed line represents ideal agreement. (b) pH correlation of the ISL and PWE techniques with mortar specimens. Dashed line represents ideal agreement.

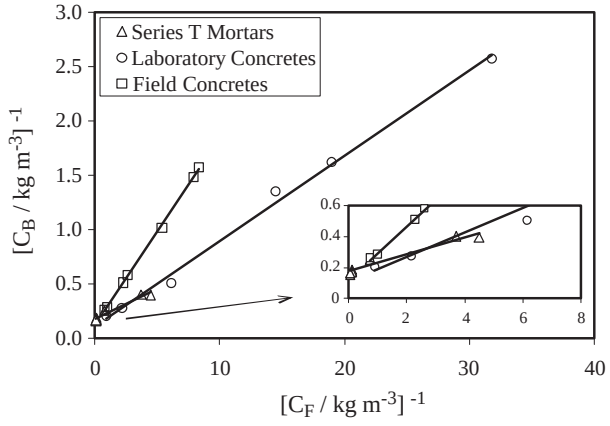

Fig. 9. Chloride binding isotherms from ISL results.

Table 8
Chloride binding parameters from ISL data and range from prior investigations using PWE

Parameter	Series T mortars	Laboratory concretes	Field concretes	Literature sources [11,14,17,26,27]
K	18	13	6	3–20
C_L (kg/m^3)	5.7	9	8.3	1.2–9.0

pH [29]) is generally considered to indicate the threshold for corrosion initiation of plain steel in atmospherically exposed concrete in the absence of extraneous polarization [30]. Thus cavities yielding results above that level would indicate corresponding risk in the immediately surrounding or similarly exposed concrete. It is noted that bound chlorides released by the cement hydration products may be available to maintain corrosion if there is a local pH decrease at the nucleating pits [31], so factors in addition to the ratio of free chloride concentration to [OH^-] may need to be considered in a detailed analysis of conditions leading to sustained reinforcement corrosion.

The results as plotted can provide insight on other concrete properties. For example, the calculated ratios follows approximately a power law of the form $C_f/[OH^-]=\alpha C_{TOT}^n$ where α is a constant for each system and n ~1.5 (concretes) to ~3 (series T mortars). The deviation from linear dependence on C_{TOT} may be interpreted as the combined effect of the presence of nonlinear binding (modeled above by a Langmuir isotherm), and decrease of pH of the cavity water [32]. As before, these examples are shown primarily as demonstration of the precision and consistency of the ISL method, which was implemented here with specimens and conditions that would have necessitated laborious preparation or been less feasible with conventional PWE.

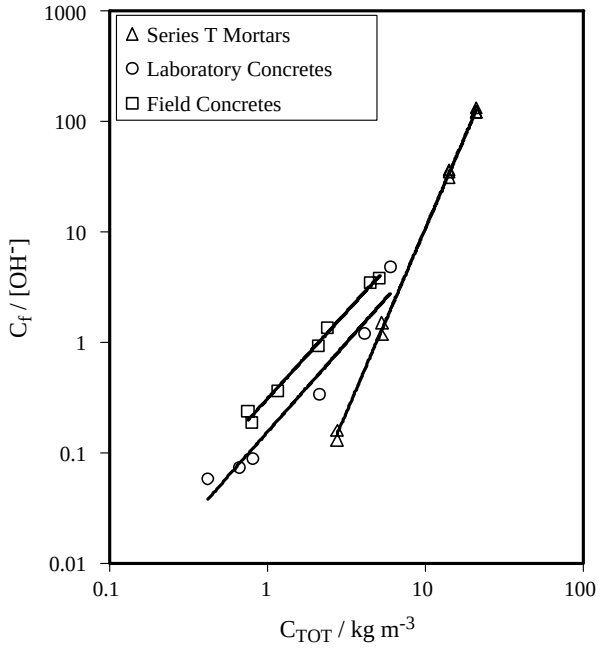

Fig. 10. Illustration of the application of ISL results to estimate chloride-to-hydroxide ratio as function of total chloride content of various materials series.

4. Conclusions

1. Modeling of the in situ leaching (ISL) process indicates that chloride binding accelerates the approach toward a terminal cavity concentration, potentially reducing test duration to practical lengths for moderate permeability concretes. For a Langmuir type absorption isotherm, the extent of acceleration is greatest in the linear binding limit at low chloride concentrations. This acceleration can be attributed to maintaining a higher gradient of C_F near the cavity wall due to the release, during leaching, of previously bound chloride.
2. The viability of the method for chloride analysis was demonstrated for laboratory mortar and concrete samples as well as for medium permeability field-extracted concrete cores. Near-equilibration times of the cavity water were attained in as short as one week. The method also provides spatial resolution for the determination of composition profiles when having total chloride concentration profile. Pore water chloride concentrations (and pH) were in close agreement with those obtained from independent high pressure pore water extraction (PWE) experiments with the same mortar materials. The present findings showed the potential of the ISL method as a viable alternative to the faster but more equipment demanding PWE method for pore water chloride determination. In the experimental examples material disruption was limited to drilling the cavities as opposed to overall crushing in a PWE test.
3. The ISL method was applied to estimate chloride ion binding isotherms and chloride-to-hydroxide values of concrete and mortar pore water. The ISL data were precise and consistent enough to permit calculation of binding model parameter values, which were within the range of typically reported results, and to consistently evaluate chloride/hydroxide ratio as function of total chloride content.
4. An occasional limitation of the ISL technique is the loss of cavity water into its surroundings, observed in some of the specimens and likely resulting from insufficient water saturation during preconditioning. In those cases cavities need periodic water replenishment, with consequent delay in achieving near-terminal concentrations. Excessive cavity water loss in extreme cases can render the method impractical.

List of Symbols

C_B	bound chloride concentration [kilogram per cubic meter of concrete]
C_F	free chloride concentration [kilogram per cubic meter of concrete]
C_f	free chloride concentration [mass per unit volume of pore water]
C_{F0}	initial free chloride concentration in concrete [kilogram per cubic meter of concrete]
C_G	generalized concentration
C_L	Langmuir adsorption coefficient [kilogram per cubic meter of concrete]
C_S	chloride concentration at the concrete surface [kilogram per cubic meter of concrete]
C_{TOT}	total chloride concentration [kilogram per cubic meter of concrete]
C_W	chloride concentration in the cavity water [M]
C_{WT}	apparent terminal chloride concentration in the cavity water [M]
C_{W0}	initial chloride concentration in the cavity water [M]
D_F	chloride diffusion coefficient for free chlorides [cm^2/s]
D_{APP}	chloride apparent diffusion coefficient [cm^2/s]
K	Langmuir adsorption coefficient
K_W	water dissociation constant
L	cavity length [cm]
pH_T	apparent terminal pH in the cavity water
r_c	cavity radius [cm]
R	generalized distance
r_e	external specimen radius [cm]
T	generalized time
t_c	concrete exposure time to salting [s]
T_D	nominal leaching time [days]
V_r	cavity volume/water volume ratio
V_C	cavity volume [cm^3]
V_W	water volume in the cavity [cm^3]
w/c	water/cement ratio
x	distance from the concrete surface exposed to salting [cm]
ε	pore volume fraction
γ_{OH}	OH^- activity coefficient

Acknowledgment

The authors are indebted to the National Science Foundation (Grant No. CMS-9872323) for the support of this investigation. The opinions and findings in this paper are those of the authors and not necessarily those of the supporting agency.

Appendix A. Assigning the Apparent Terminal Chloride Concentration Value to a Data Series

The experimental results for any leaching experiment span a finite time interval during which C_{WT} is approached but not reached. In principle, the data set could be compared with the output of the model developed here, and then varying C_{WT} and the other model parameters until a best fit criterion is satisfied. The procedure would then yield an extrapolated value of C_{WT} as well as of the other parameter values. However, no straightforward procedure to do that has been developed at present and it is not clear whether the procedure would be sufficiently valid considering the many simplifying modeling assumptions made. Instead, a compromise approach was used in which the leaching experiments were extended until a plateau began to be apparent in a log C_W-log time graph. To minimize operator judgment in calculating a C_{WT} value from the plateau portion of the graph (which would involve deciding which data points from earlier times to leave out in obtaining the average in the plateau region), the following procedure was adopted. From the model output curves in Fig. 2, a simplified idealized output was abstracted consisting of a two consecutive straight lines in the log–log representation. The first line has a slope of 1/2 (approximating the

early diffusional regime) while the second has a slope of zero at an ordinate value log C_{WT} where C_{WT} is understood to be a nominal approximation of the actual terminal value. Both lines joint at an abscissa value log T_D, where T_D is a nominal equilibration time.

The values of C_{WT} and T_D can be obtained independent of operator judgment (other than the decision as to whether a plateau regime has been entered) by the following fitting procedure, using a least square error sum criterion. Calling (t_i, C_{Wi}) with $i=1$ to n the n available experimental time and concentration pairs for a test series, the fit function is then:

$$f(\log t, \log C_{WT}, \log T_D) = \left(\log C_{WT} - \frac{\log T_D - \log t_i}{2}\right) \mathrm{IF}(A) + \log C_{WT}\,\mathrm{IF}(B) \quad \text{(A1)}$$

with $A=\log t_i < \log T_D$, $B=\log t_i \geq \log T_D$, and the IF operator equals 1 if the condition is true and 0 otherwise.

The simplified fitting procedure consisted then of minimizing:

$$\sum_{i=1}^{n} \left(C_{Wi} - f(\log t_i, \log C_{WT}, \log T_D)\right)^2 \quad \text{(A2)}$$

by the Levenberg–Marquardt method, which is available in commonly used software packages. The procedure was successfully applied to the data sets in Figs. 5, 6, and 7 and the resulting fit functions are shown there as well.

References

[1] S. Nagataki, N. Otsuki, T. Wee, K. Nakashita, Condensation of chloride ion in hardened cement matrix materials and on embedded steel bars, ACI Mater. J. 90 (4) (1993) 323–332.

[2] G.K. Glass, N.R. Buenfeld, in: L.O. Nilsson, J.P. Olliiner (Eds.), The determination of chloride binding relationships on proceedings of the International RILEM Publications Workshop, France, 3-9, 1995.

[3] P. Nixon, C.L. Page, Pore solution chemistry and alkali aggregate reaction, in: J.M. Scanlon (Ed.), Concrete Durability on Katharine and Bryant Mather International Conference, ACI SP 100-94, 1987, pp. 1833–1862.

[4] J. Tritthard, Chloride binding in cement: investigations to determine the composition of porewater in hardened cement, Cem. Concr. Res. 19 (4) (1989) 586–594.

[5] M. Castellote, C. Alonso, C. Andrade, P. Castro, M. Echevarría, Alkaline leaching method for the determination of the chloride content in the aqueous phase of hardened cementitious materials, Cem. Concr. Res. 31 (2) (2001) 233–238.

[6] A.A. Sagüés, E.I. Moreno, C. Andrade, Evolution of pH during in-situ leaching in small concrete cavities, Cem. Concr. Res. 27 (11) (1998) 1747–1759.

[7] L. Li, A.A. Sagüés, N. Poor, In-situ leaching investigation of pH and nitrite concentration in concrete pore solution, Cem. Concr. Res. 29 (3) (1999) 315–321.

[8] P.D. Cady, R.E. Weyers, Deterioration rules of concrete bridge decks, Journal of Transportation Engineering, 110 (1), American Society of Civil Engineers, 1984, pp. 35–44.

[9] P. Bamforth, Admitting that Chlorides are Admitted, Concrete Magazine, Nov/Dec 1994, p. 18.

[10] A.A Sagüés, S.C. Kranc, Effect of structural shape and chloride binding on time to corrosion of steel in concrete in marine service, in: C.L. Page, P.B. Bamforth, J.W. Figg (Eds.), Corrosion of Reinforcement in Concrete Construction, The Royal Society of Chemistry, Cambridge, 1996, pp. 105–114.

[11] Rasheeduzzafar, S. Ehtesham Hussain, S.S. Al-Saadoun, Effect of cement composition on chloride binding and corrosion of reinforcing steel in concrete, Cem. Concr. Res. 21 (5) (1991) 777–794.

[12] O.L. Nilsson, M.T. Massa, L. Tang, The effect of non-linear chloride binding on the prediction of chloride penetration into concrete structures, in: V.M. Malhotra (Ed.), Durability of Concrete, ACI Publication SP-145, American Concrete Institute, Detroit, 1994, p. 469.

[13] S. Nagataki, N. Otsuki, W. Tiong-Huan, K. Nagashita, Condensation of chloride ion in hardened cement matrix materials and on embedded steel bars, ACI Mater. J. 90 (1992) 323–332.

[14] Rasheeduzzafar, S. Hussain, S.S. Saadoun, Effect of tricalcium aluminate content of cement on chloride binding and corrosion of reinforcing steel in concrete, ACI Mater. J. 89 (1) (1992) 3–12.

[15] J. Tritthart, Chloride binding in cement: II — The influence of the hydroxide concentration in the pore solution of hardened cement paste on chloride binding, Cem. Concr. Res. 19 (5) (1989) 683–691.

[16] C. Arya, Y. Xu, Effect of cement type on chloride binding and corrosion of steel in concrete, Cem. Concr. Res. 25 (4) (1995) 893–902.

[17] L. Tang, L.O. Nilsson, Ibid 23 (1993) 247–253.

[18] J. Crank, The Mathematics of Diffusion, 2nd ed.Oxford University Press, Oxford, 1975.

[19] R.E. Weyers, Concrete Bridge Protection, Repair and Rehabilitation Relative to Reinforcement Corrosion: A Methods Application Manual, SHRP-S-360, National Research Council, Washington, DC, 1993.

[20] N.S. Berke, M.C. Hicks, Estimating the life cycle of reinforced concrete decks and marine piles using laboratory diffusion and corrosion data, in: Victor Chacker (Ed.), Corrosion Forms and Control for Infrastructure, ASTM STP, vol. 1137, American Society for Testing and Materials, Philadelphia, 1992, p. 207.

[21] R.J. Kessler, V.E. Arrebola, R.S. Lingerfelt, R.P Brown, Determination of Low-Levels of Chloride in Concrete and Raw Materials, Research Report, 203, Florida Department of Transportation, Office of Materials and Research, 1978.

[22] R.S. Barneyback, S. Diamond, Expression and analysis of pore fluids from hardened cement pastes and mortars, Cem. Concr. Res. 11 (2) (1981) 279–285.

[23] VDOT, Road and Bridge Specifications, Virginia Department of Transportation, Richmond, 1991.

[24] A.A. Sagüés, Modeling the effects of corrosion on the lifetime of extended reinforced concrete structures, Corrosion 59 (2003) 854.

[25] S. Goñi, A. Moragues, C. Andrade, Influence of the conductivity and the ionic strength of synthetic solutions which simulate the aquose phase of concrete in the corrosion process, Mater. Constr. 39 (215) (1989).

[26] M.N. Haque, O.A. Kayyali, Cem. Concr. Res. 25 (3) (1995) 531–542.

[27] C.J. Pereira, L.L. Hegedus, Diffusion and Reaction of Chloride Ions in Porous Concrete, Chemical Reaction Engineering, Eighth International Symposium Series, vol. 87, 1984.

[28] R.M. Pytkowicz, Activity Coefficients in Electrolyte Solutions, vol. 2, CRC Press, Boca Raton, Florida, 1979.

[29] L. Li, A.A. Sagüés, Chloride corrosion threshold of reinforcing steel in alkaline solutions—open-circuit immersion tests, Corrosion 57 (2001) 19.

[30] F.J. Presuel-Moreno, A.A. Sagüés, S.C. Kranc, Steel activation in concrete following interruption of long term cathodic polarization, Corrosion 61 (5) (2005) 428–436.

[31] G.K. Glass, B. Reddy, N.R. Buenfeld, The participation of bound chloride in passive film breakdown on steel in concrete, Corros. Sci. 42 (2000) 2013–2021.

[32] B. Martin Perez, H. Zibara, R.D. Hooton, M.A.D. Thomas, A study of the effect of chloride binding on service life prediction, Cem. Concr. Res. 30 (8) (2000) 1215–1223.